Identifying Task-Based Dynamic Functional Connectivity Using Tensor Decomposition

Wenya Liu[1,2], Xiulin Wang[1,2], Tapani Ristaniemi[2], and Fengyu Cong[1,2,3,4](✉)

[1] School of Biomedical Engineering, Faculty of Electronic Information and Electrical Engineering, Dalian University of Technology, 116024 Dalian, China
wenyaliu0912@foxmail.com, xiulin.wang@foxmail.com, cong@dlut.edu.cn
[2] Faculty of Information Technology, University of Jyväskylä, Jyväskylä, Finland
tapani.e.ristaniemi@jyu.fi
[3] School of Artificial Intelligence, Faculty of Electronic Information and Electrical Engineering, Dalian University of Technology, 116024 Dalian, China
[4] Key Laboratory of Integrated Circuit and Biomedical Electronic System, Dalian University of Technology, 116024, Liaoning, Dalian, China

Abstract. Functional connectivity (FC) patterns in human brain are dynamic in a task-specific condition, and identifying the dynamic changes is important to reveal the information processing processes and network reconfiguration in cognitive tasks. In this study, we proposed a comprehensive framework based on high-order singular value decomposition (HOSVD) to detect the stable change points of FC using electroencephalogram (EEG). First, phase lag index (PLI) method was applied to calculate FC for each time point, constructing a 3-way tensor, i.e., connectivity × connectivity × time. Then a stepwise HOSVD (SHOSVD) algorithm was proposed to detect the change points of FC, and the stability of change points were analyzed considering the different dissimilarity between different FC patterns. The transmission of seven FC patterns were identified in a task condition. We applied our methods to EEG data, and the results verified by prior knowledge demonstrated that our proposed algorithm can reliably capture the dynamic changes of FC.

Keywords: Dynamic functional connectivity · HOSVD · EEG · Tensor decomposition

1 Introduction

Brain functional connectivity (FC) is essentially dynamic for different cognitive demands even in a task-specific condition, and identifying the changes of FC can help to understand the reconfiguration of brain network topology along cognitive tasks [3,6,11]. Electroencephalogram (EEG) can record the electrical brain activity in a millisecond timescale with low cost, and this temporal richness shines new light to the dynamic FC analysis in a specific cognitive task which presents short and repeated stimuli, like stimuli used in event-related potential (ERP) study. It is important to find the task-locked dynamic brain networks to

H. Yang et al. (Eds.): ICONIP 2020, CCIS 1333, pp. 361–369, 2020.
https://doi.org/10.1007/978-3-030-63823-8_42

explore the precise brain topology changes in information processing. For ERP study, traditional methods calculate static FC for the whole trial which can not accurately capture the real reconfiguration of brain networks regarding the stimuli. Based on the fact that moment-to-moment fluctuations in FC are more stable during task than rest [6], pinpointing the time intervals during which the FC is considered stationary is in line with reality under task-specific condition.

Existing methods for dynamic FC are mainly based on sliding window, which segment the whole time series into a number of overlapping time windows, then community detection, clustering and graph theory-based methods are applied to evaluate the FC evolutions across time windows [1,2,5,15]. But this kind of methods are sensitive to the choice of window length, overlapping and window shape [9]. Another category of commonly used methods are based on matrix factorization, like temporal principal component analysis (PCA) and temporal independent component analysis (ICA) [10,13], which decompose the data (time $\times$ connectivity) into connectivity components and the corresponding temporal profile. However, the uncorrelated or independent constraint imposed to connectivity components is not practical into use.

Recently, tensor decomposition methods are applied to dynamic FC analysis [11,12] for change point detection, which can take the multiway arrangement of connectivity along time, frequency and subject dimensions into consideration. Inspired by their works, which used high-order singular value decomposition (HOSVD) for the analysis of dynamic FC, in this study, we constructed a 3-way tensor formed by connectivity matrix along time (connectivity $\times$ connectivity $\times$ time), and proposed a comprehensive framework to detect the change points of brain networks in an ERP dataset. Our work is different from the previous studies in [11,12] with some new highlights. First, we proposed a stepwise HOSVD (SHOSVD) method to detect the dynamic changes sequentially and avoid spurious FC changes caused by outliers. Second, we combined the results from a range of parameters to obtain multiple sets of stable change points, allowing different dissimilarity between different pairs of FC patterns, so the results are not sensitive to the predefined threshold of FC dissimilarity measurement. Our proposed algorithm can efficiently track the dynamic changes of brain networks during task condition, and its feasibility is demonstrated by an ERP study.

2 Materials and Methods

2.1 Data Description

Our proposed framework was applied to EEG data which have been published in [7,16]. In this experiment, nineteen participants were informed to play a three-agent ("Self", another participant called "Other", and a computer called "Computer") gambling game, and two golden eggs were presented to choose by each agent. After the choice of a golden egg, a cue stimuli was presented which indicated whether the participants will be informed about the outcomes such that curiosity will be satisfied (CWS) or curiosity will not be satisfied (CWN), then the feedback of monetary gain or loss was given.

The data were collected at 64 scalp sites using the electrodes mounted in an elastic cap (Brain Product, Munich, Germany), and preprocessed using EEGLAB [4]. One participant was removed due to bad data quality, and data were down-sampled to 500 Hz and band-pass filtered to 1–40 Hz. Eye movements were rejected by ICA, and the cue-locked data were extracted from −200 ms to 1000 ms. Then any segment whose max amplitude exceeds 100 μV was removed.

According to the results of previous paper [16], we only analyzed the data of cue onset in Self and CWS condition, and 58 scalp channels were used in this study.

2.2 Phase Synchronization

The communication of brain regions or neural populations depends on phase interactions for electrophysiological neuroimaging techniques, like EEG [17]. Considering the volume conduction effect to sensor space connectivity, we calculated the pairwise synchronization using PLI which can avoid volume conduction effect by discarding zero-lag interactions [14].

For signal $x(t)$, $t = 1, 2, \cdots, T$, its analytical signal $z(t)$ can be constructed by Hilbert transform,

$$z(t) = x(t) + i\tilde{x}(t) = \frac{1}{\pi} PV \int_{-x}^{\infty} \frac{x(\tau)}{t-\tau} d_\tau, \tag{1}$$

where $\tilde{x}(t)$ is the imaginary part and PV refers to the Cauchy principal value. Then the instantaneous phase $\varphi(t)$ can be computed as follows:

$$\varphi(t) = arctan \frac{\tilde{x}(t)}{x(t)}. \tag{2}$$

For an ERP dataset containing C channels, S subjects and N trials, the phase synchronization between channel i and channel j at time t for subject s can be computed by PLI:

$$PLI^s_{(i,j)}(t) = \frac{1}{N} \left| \sum_{n=1}^{N} sign(\Delta\varphi^s_{(i,j,n)}) \right|, \tag{3}$$

where $\Delta\varphi^s_{(i,j,n)} = \varphi^s_{(i,n)} - \varphi^s_{(j,n)}$ is the phase difference between channel i and channel j at time t for subject s. It should be noted that any 0 or $\pm\pi$ value of $\Delta\varphi^s_{(i,j,n)}$ is discarded here which is considered to be caused by volume conduction.

In our study, the PLI value is calculated by averaging across trials and subjects, because that phase synchrony can only be detected in a statistical sense. We also assume that the phases at time t are the same for all subjects due to the stimulus-locked EEG. Then we can get the time-varying adjacency matrix at time point t:

$$\boldsymbol{A}_{(i,j)}(t) = \frac{1}{S} \sum_{s=1}^{S} PLI^s_{(i,j)}(t), \tag{4}$$

where $\boldsymbol{A}(t) \in \mathbb{R}^{C\times C}$, and a nonnegative FC tensor of connectivity × connectivity × time can be constructed as $\boldsymbol{\mathcal{A}} \in \mathbb{R}^{C\times C\times T}$.

2.3 Stepwise High-Order Singular Value Decomposition

HOSVD is a tensor generalization of singular value decomposition (SVD) with orthogonal factors in each mode. Each factor matrix is computed by the left singular vectors of SVD performed on the unfolded tensor along the corresponding mode, such as the factor in mode 3:

$$\boldsymbol{A}_3 = \boldsymbol{U}_{time}\boldsymbol{D}\boldsymbol{V}^T, \tag{5}$$

where $\boldsymbol{A}_3 \in \mathbb{R}^{T\times CC}$ is mode 3 matricization of tensor $\boldsymbol{\mathcal{A}}$, $\boldsymbol{D} \in \mathbb{R}^{T\times CC}$ is the diagonal matrix, and $\boldsymbol{V} \in \mathbb{R}^{CC\times CC}$ is the right singular vectors. The FC tensor $\boldsymbol{\mathcal{A}} \in \mathbb{R}^{C\times C\times T}$ is fully decomposed using HOSVD:

$$\boldsymbol{\mathcal{A}} = \boldsymbol{\mathcal{G}} \times_1 \mathbf{U_{conn}} \times_2 \mathbf{U_{conn}} \times_3 \mathbf{U_{time}}, \tag{6}$$

where $\boldsymbol{\mathcal{G}} \in \mathbb{R}^{C\times C\times T}$ is the core tensor, $\boldsymbol{U}_{conn} \in \mathbb{R}^{C\times C}$ and $\boldsymbol{U}_{time} \in \mathbb{R}^{T\times T}$ are the factor matrices in connectivity space and time space, respectively. Note that the factor matrices in mode 1 and mode 2 are the same because of the symmetry of connectivity matrix $\boldsymbol{A}(t)$, and the core tensor $\boldsymbol{\mathcal{G}}$ represents the interactions between 3 modes.

Let $\boldsymbol{\mathcal{A}}^{time}$ denote the multiplication of tensor $\boldsymbol{\mathcal{A}} \in \mathbb{R}^{C\times C\times T}$ with the factor matrix $\boldsymbol{U}_{time} \in \mathbb{R}^{T\times T}$ in mode 3, so we can get:

$$\boldsymbol{\mathcal{A}}^{time} = \boldsymbol{\mathcal{A}} \times_3 \boldsymbol{U}_{time}^T, \tag{7}$$

Then we can get the first frontal slice:

$$\boldsymbol{A}_{:,:,1}^{time} = \sum_{t=1}^{T} u_{t,1}^{time} \boldsymbol{A}_{:,:,t}, \tag{8}$$

where $u_{t,1}^{time}$ denotes the tth element in the first column of factor matrix $\boldsymbol{U}_{time}$, and $\boldsymbol{A}_{:,:,t}$ means the tth frontal slice of the original tensor $\boldsymbol{\mathcal{A}}$. Because factor matrix $\boldsymbol{U}_{time}$ is the left singular vectors of SVD performed on nonnegative matrix $\boldsymbol{A}_{(3)}$, so elements of the first column $u_{:,1}^{time}$ are all positive or all negative, i.e., they have the same sign. So we can regard the first frontal slice $\boldsymbol{A}_{:,:,1}^{time}$ as the weighted sum of connectivity across time, and this is also called the summarization of the stationary connectivity in a time interval [12]. On the other hand, $\boldsymbol{A}_{:,:,1}^{time}$ captures most of the energy of time-varying connectivity patterns across the stationary time interval, due to that the corresponding singular value of $u_{:,1}^{time}$ is the largest one. Considering the superiority described above, we proposed a SHOSVD algorithm for dynamic FC change points detection, as illustrated below.

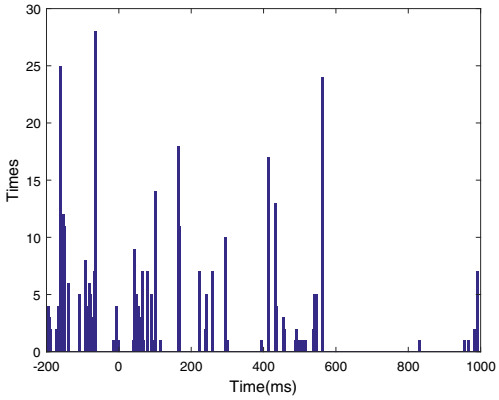

Fig. 1. The times of each time point detected as change point. 82 time points are detected as change points in 51 runs of SHOSVD.

Summary of the proposed SHOSVD algorithm:

Step 1: Set $t = 3$, and perform full HOSVD on the tensor $\tilde{\boldsymbol{\mathcal{A}}} \in \mathbb{R}^{C\times C\times t}$ constructed by the first t frontal slices of original FC tensor $\boldsymbol{\mathcal{A}}$.

Step 2: Compute the absolute value of the first frontal slice $\tilde{\boldsymbol{A}}^{time}_{:,:,1}(t)$, and normalize it to [0 1].

Step 3: Normalize the consequent three original FC matrices $\boldsymbol{\mathcal{A}}_{:,:,t+1}$, $\boldsymbol{\mathcal{A}}_{:,:,t+2}$ and $\boldsymbol{\mathcal{A}}_{:,:,t+3}$ to [0 1], respectively.

Step 4: Compute Euclidean distance ρ_1, ρ_2 and ρ_3 between $\tilde{\boldsymbol{A}}^{time}_{:,:,1}(t)$ and $\boldsymbol{\mathcal{A}}_{:,:,t+1}$, $\boldsymbol{\mathcal{A}}_{:,:,t+2}$ and $\boldsymbol{\mathcal{A}}_{:,:,t+3}$, respectively.

Step 5: Compare ρ_1, ρ_2 and ρ_3 with the predefined threshold λ.

Step 6: If $\rho_1 > \lambda$ & $\rho_2 > \lambda$ & $\rho_3 > \lambda$, save t as the change point for the sub-segment, remove $\tilde{\boldsymbol{\mathcal{A}}} \in \mathbb{R}^{C\times C\times t}$ from original FC tensor $\boldsymbol{\mathcal{A}}$, and go back to step 1. Else, set $t = t + 1$, and go back to step 1.

The detection will be terminated until all the time points are included to a stationary interval. Here we give some statements about the proposed SHOSVD algorithm. In step 1, we start the algorithm with $t = 3$ for the conduction of HOSVD, because we assume that the first three time points are in the same stationary segment. In step 2, the first frontal slice $\tilde{\boldsymbol{A}}^{time}_{:,:,1}(t)$ should be all negative or all positive due to the uncertain sign of $u^{time}_{:,1}$, so here we take its absolute value for the following analysis. In step 2 and step 3, the normalization is necessary to constraint the matrices to the same scale, because we focus on the similarity between connectivity patterns which should not be affected by their amplitude scales. For a matrix $\boldsymbol{X}$, the normalization is realized by $\tilde{x}_{ij} = \frac{x_{ij}-min(X)}{max-min(X))}$, so all the elements are constrained to [0 1], which is the classical range of a FC matrix. In step 4, the Euclidean distance is computed by the L_2 norm of the difference between two matrices. In step 6, we test the distances for the consequent three time points to avoid spurious changes by outliers. In step 5, the predefined threshold λ is the only parameter to be determined in SHOSVD method, and its selection will be discussed in the next section.

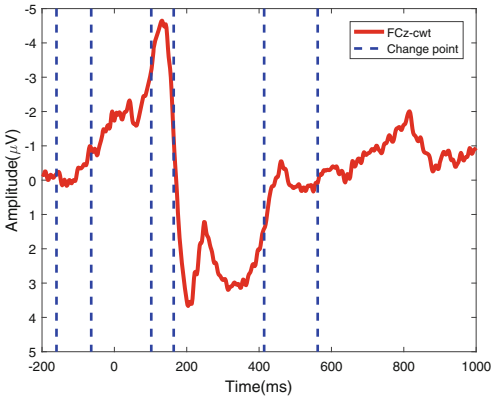

Fig. 2. The stable change points of dynamic functional connectivity. The red line represents the grand averaged data across trials and subjects of FCz channel. The blue dotted lines mean the change points located at −160 ms, −64 ms, 102 ms, 164 ms, 414 ms, and 562 ms. (Color figure online)

2.4 The Stability of Change Points

Considering the fact that the dissimilarity of various pairs of FC patterns may be different. For example, the distance ρ_{12} between connectivity patterns 1 and 2 is undoubtedly different from the distance ρ_{23} between connectivity patterns 2 and 3, because different connectivity patterns may share the same connections, like visual network and frontal-visual network, or share none connections, like visual network and frontal network. So we can not set a common threshold for the change point evaluation. Here we set a range of threshold $[\lambda_1 \ \lambda_2]$ which would be determined with experience by testing the performance of SHOSVD on the data, and perform SHOSVD for each threshold λ in the predefined range. After obtaining the multiple sets of change points, we take the most frequently appeared points as the final stable change points, which are considered to characterize the time-varying FC changes. Therefore, the results are not sensitive to the choice of threshold.

3 Results

3.1 Change Points Detection

First, PLI method was performed on the preprocessed data at each time point, constructing a 3-way FC tensor with dimensions of 58 × 58 × 600. Then SHOSVD was applied for change points detection. Dissimilarity thresholds were selected between the range with a step of 0.1, so 51 sets of change points were obtained in this study. All the change points detected for the 51 runs of SHOSVD were shown in Fig. 1. Finally, we kept 10% of the most frequently appeared time points as the final stable change points which can characterize the dynamic FC

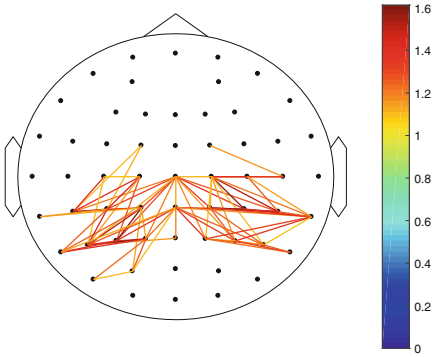

Fig. 3. The brain network summarization of stationary time interval (164–414) ms.

variety, as shown in Fig. 2. From the red line of Fig. 2, we can see that the cue stimuli induced a feedback-related negativity (FRN)-like component followed by a P300 component. Refer to [16] for a detailed explanation. According to Eqs. (6–8), we summarize the FC in time interval (164–414) ms. Figure 3 and Fig. 4 depicted the brain network and connectivity matrix of stationary time interval (164–414) ms which contained both FRN-like component and P300 component, respectively. We obtained a central-posterior network which was consistent with the previous findings [16].

3.2 Discussion

Previous studies have reported that curiosity is a type of reward anticipation which can induce a FRN-like component, and a following P300 component which is associated with context updating and behavioral adjustments [8,16,18]. In our results, we incorporated both FRN-like and P300 components into the same stable time interval (164–414) ms, and summarized a central-posterior functional connectivity. In the previous results, a central-posterior delta power was elicited by the cue stimuli within 200–350 ms, and the brain activation results were consistent with our findings [16]. From our results, we conclude that the curiosity satisfaction and behavioral adjustment may share the same brain topology configuration. However, this interpretation needs further verification which should take the FC variety across frequency domain into consideration. What's more, other stable time intervals also need to be deeply analyzed, which is our future extended work based on this study. The number of change points should be verified by prior knowledge which is important to the explanation of the results.

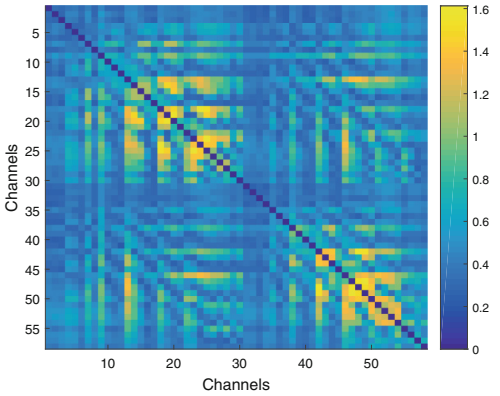

Fig. 4. The connectivity matrix summarization of stationary time interval (164–414) ms.

4 Conclusion

In this study, we proposed a comprehensive framework for the analysis of task-based dynamic FC. Tensor decomposition technique is applied considering the multiway arrangement of connectivity matrices across time, so both structure properties of FC and its variety information along time are considered for the change points detection. As we all know, it is hard and important to exactly lock the brain response to external stimuli and characterize the changes of brain states in a specific cognitive task. Our change points detection framework can efficiently separate different brain topology configurations in a task condition.

Acknowledgments. This work was supported by National Natural Science Foundation of China (Grant No. 91748105), National Foundation in China (No. JCKY2019110B009), the Fundamental Research Funds for the Central Universities [DUT2019] in Dalian University of Technology in China, and the scholarships from China scholarship Council (No. 201706060263 & No. 201706060262). The authors would like to thank Dr. Peng Li for the provide of EEG data and Guanghui Zhang for the preprocessing work.

References

1. Allen, E.A., Damaraju, E., Plis, S.M., Erhardt, E.B., Eichele, T., Calhoun, V.D.: Tracking whole-brain connectivity dynamics in the resting state. Cereb. Cortex **24**(3), 663–676 (2014)
2. Bassett, D.S., Wymbs, N.F., Porter, M.A., Mucha, P.J., Carlson, J.M., Grafton, S.T.: Dynamic reconfiguration of human brain networks during learning. Proc. Nat. Acad. Sci. **108**(18), 7641–7646 (2011)
3. Cohen, J.R.: The behavioral and cognitive relevance of time-varying, dynamic changes in functional connectivity. NeuroImage **180**, 515–525 (2018)

4. Delorme, A., Makeig, S.: Eeglab: an open source toolbox for analysis of single-trial eeg dynamics including independent component analysis. J. Neurosci. Methods **134**(1), 9–21 (2004)
5. Dimitriadis, S.I., Laskaris, N.A., Tsirka, V., Vourkas, M., Micheloyannis, S., Fotopoulos, S.: Tracking brain dynamics via time-dependent network analysis. J. Neurosci. Methods **193**(1), 145–155 (2010)
6. Gonzalez-Castillo, J., Bandettini, P.A.: Task-based dynamic functional connectivity: recent findings and open questions. Neuroimage **180**, 526–533 (2018)
7. Han, C., Li, P., Warren, C., Feng, T., Litman, J., Li, H.: Electrophysiological evidence for the importance of interpersonalcuriosity. Brain Res. **1500**, 45–54 (2013)
8. Kang, M.J., et al.: The wick in the candle of learning: epistemic curiosity activates reward circuitry and enhances memory. Psychol. Sci. **20**(8), 963–973 (2009)
9. Khambhati, A.N., Sizemore, A.E., Betzel, R.F., Bassett, D.S.: Modeling and interpreting mesoscale network dynamics. NeuroImage **180**, 337–349 (2018)
10. Leonardi, N., et al.: Principal components of functional connectivity: a new approach to study dynamic brain connectivity during rest. NeuroImage **83**, 937–950 (2013)
11. Leonardi, N., Van De Ville, D.: Identifying network correlates of brain states using tensor decompositions of whole-brain dynamic functional connectivity. In: 2013 International Workshop on Pattern Recognition in Neuroimaging, pp. 74–77. IEEE (2013)
12. Mahyari, A.G., Zoltowski, D.M., Bernat, E.M., Aviyente, S.: A tensor decomposition-based approach for detecting dynamic network states from EEG. IEEE Trans. Biomed. Eng. **64**(1), 225–237 (2016)
13. O'Neill, G.C., et al.: Measurement of dynamic task related functional networks using MEG. NeuroImage **146**, 667–678 (2017)
14. Stam, C.J., Nolte, G., Daffertshofer, A.: Phase lag index: assessment of functional connectivity from multi channel eeg and meg with diminished bias from common sources. Hum. Brain Mapp. **28**(11), 1178–1193 (2007)
15. Valencia, M., Martinerie, J., Dupont, S., Chavez, M.: Dynamic small-world behavior in functional brain networks unveiled by an event-related networks approach. Phys. Rev. E **77**(5), 050905 (2008)
16. Wang, J., et al.: To know or not to know? theta and delta reflect complementary information about an advanced cue before feedback in decision-making. Front. Psychol. **7**, 1556 (2016)
17. Womelsdorf, T., et al.: Modulation of neuronal interactions through neuronal synchronization. Science **316**(5831), 1609–1612 (2007)
18. Wu, Y., Zhou, X.: The p300 and reward valence, magnitude, and expectancy in outcome evaluation. Brain Res. **1286**, 114–122 (2009)